American Mineralogist, Volume 92, pages 560–569, 2007

Low-temperature behavior of $NaGaSi_2O_6$

F. Nestola,[1,*] N. Rotiroti,[2,†] M. Bruno,[3] M. Tribaudino,[4] S. van Smaalen,[2] H. Ohashi,[5] and G.J. Redhammer[6]

[1]Bayerisches Geoinstitut, University of Bayreuth, D-95440, Bayreuth, Germany
[2]Laboratory of Crystallography, University of Bayreuth, D-95440, Bayreuth, Germany
[3]Dipartimento di Scienze Mineralogiche e Petrologiche, Università di Torino, Via Valperga Caluso 35, I-10125, Torino, Italy
[4]Dipartimento di Scienze della Terra, Università di Parma, Parco Area delle Scienze 157/A, 43100 Parma, Italy
[5]HASHI Institute for Silicate Science Nishinakanobu, 1-9-25, Shinagawa, Tokyo 142-0054, Japan
[6]Institute of Crystallography, University of Technology, Rheinisch-Westfälische 11 Technische Hochschule Aachen, Jägerstrasse 17/19, D-52056 Aachen, Germany

Abstract

Synthetic $NaGaSi_2O_6$-pyroxene, space group $C2/c$, was investigated at low temperature between 295 to 110 K by X-ray diffraction. The evolution of the unit-cell parameters as a function of temperature does not indicate any structural phase transition down to 110 K. Calculated values for the Debye temperature, θ_D, and the Grüneisen parameter, γ, are 653(39) and 0.84(8) K, respectively, close to those of other pyroxenes. Five complete intensity data collections were performed at 295, 235, 190, 145, and 110 K to investigate the temperature dependence of the crystal structure. The space group remains $C2/c$ down to 110 K, but anomalies were found between 235 and 190 K for the temperature dependencies of the volume and strain of the M1 polyhedron. This anomalous behavior could be related to variations of the Ga-O2(C1,D1) bond length and the O1(A1,B1)-Ga-O2(C1,D1) bond angle. The $C2/c$-$P\bar{1}$ phase transition observed in a previous work for $NaTiSi_2O_6$ at about 200 K did not occur for $NaGaSi_2O_6$ down to the minimum temperature investigated in this work. This is not due to the different ionic radius at M1 site or to a different tetrahedral chain extension between these two compositions but it is likely due to unfilled t_{2g} orbitals, which do not exist in $NaGaSi_2O_6$.

Keywords: Clinopyroxene, crystal structure, X-ray diffraction, low temperature

Introduction

Na-clinopyroxenes are among the most studied silicates because of their abundance in the Earth's lower-crust and upper mantle. They are major constituents of important high-pressure rocks (e.g., blueschists, eclogites) and are involved in several chemical reactions (e.g., $NaAlSi_3O_8 = NaAlSi_2O_6 + SiO_2$) crucial for the understanding the Earth's constitution. Na-clinopyroxenes have the general chemical formula $NaM^{3+}Si_2O_6$, with M = Al, Ga, In, Sc, Ti, V, Cr, Mn, and Fe, and space group $C2/c$ at room conditions (Prewitt and Burnham 1966; Clark et al. 1969; Cameron et al. 1973; Hawthorne and Grundy 1974; Ohashi et al. 1982, 1983, 1987, 1990, 1994a, 1994b, 1995; Redhammer et al. 2003). The $C2/c$ pyroxene crystal structure, which has been described in several previous works (see as a reference Yang and Prewitt 2000), is illustrated in Figure 1.

Several investigations have been performed on Na-pyroxenes as a function of temperature and pressure (Zhao et al. 1997; Redhammer and Roth 2002; Origlieri et al. 2003; Redhammer et al. 2003, 2006; Tribaudino et al. 2005; Nestola et al. 2006). However, in spite of their simple crystal structures, some anomalous behavior is still to be clarified. It is, for instance, almost completely unknown whether a change of the electronic environment (e.g., changes in bond character, high-low spin transitions, crystal field effects) around the M1 site can affect significantly the pyroxene structure. It has been observed that some $NaM^{3+}Si_2O_6$ clinopyroxenes with the same composition but synthesized under different conditions, show small but significant differences in densities and crystal structures at ambient conditions ($NaTiSi_2O_6$, Ohashi et al. 1982 and Redhammer et al. 2003; $NaInSi_2O_6$, Hawthorne and Grundy 1974 and Ohashi et al. 1990; $NaGaSi_2O_6$, Ohashi et al. 1983, 1995). Some authors have attributed such density variations to different electronic states of the M^{3+} ion (Ohashi et al. 1995). For instance, X-ray diffraction investigations at room temperature on a sample with Ga at the M1 site, $NaGaSi_2O_6$, showed the presence of two different structural configurations around the octahedral Ga^{3+} ion: Ga(α) and Ga(β) (Ohashi et al. 1983, 1995). $NaGa(\alpha)Si_2O_6$ has a denser structure than $NaGa(\beta)Si_2O_6$ (3.91 and 3.89 Mg/m^3, respectively) and a smaller M1 polyhedral volume [10.18(4) Å^3 vs. 10.289(6) Å^3]. The $NaGa(\alpha)Si_2O_6$ compound has been quenched from high-pressures and temperatures more slowly than $NaGa(\beta)Si_2O_6$. It was assumed that the α and β forms represent two different polymorphs, possibly differing in the electronic state of the Ga-cation (Ohashi et al. 1995).

$NaGaSi_2O_6$ is not the only Ga-bearing compound showing

* Present address: Dipartimento di Geoscienze, Università di Padova, Corso Garibaldi 37, I-35137, Padova, Italy. E-mail: fabrizio.nestola@unipd.it
† Present address: Dipartimento di Scienze della Terra, Università di Milano, Via Botticelli 23, I-20133, Milano, Italy.

0003-004X/07/0004–560$05.00/DOI: 10.2138/am.2007.2304

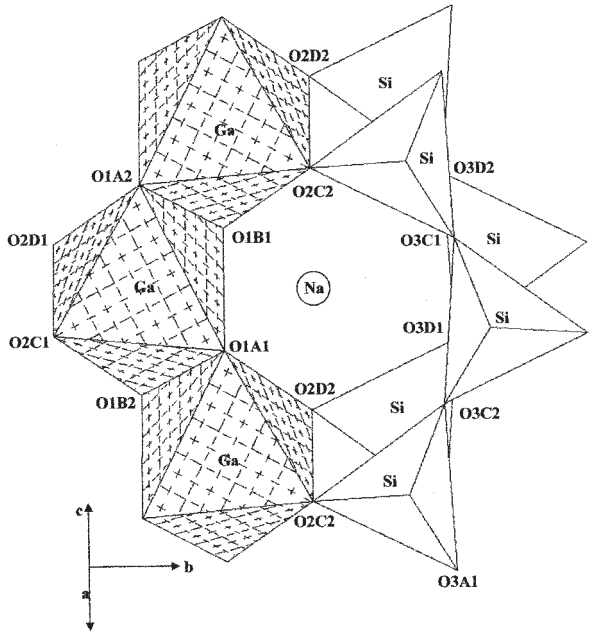

FIGURE 1. Projection of the structure of $NaGaSi_2O_6$ onto the (100) plane at room temperature. Atom labeling follows Clark et al. (1969).

anomalous behavior, as demonstrated by previous investigations on $GaPO_4$ (Sowa 1994) and $La_3Ga_5SiO_{14}$ (Werner et al. 2002). A recent investigation on $PrGaO_3$ (Vasylechko et al. 2005, orthorhombic with perovskite-type structure), using single-crystal X-ray diffraction, shows a yet unexplained change in slope in the Ga-Ga average distances between 200 and 300 K. The above anomalous behavior is revealed by very small structural variations, which might be hidden in the noise of less precise experiments. However, modern diffractometers allow us to determine such small differences, which were previously undetectable. Furthermore, with measurements at low temperature, the reduced thermal displacements permit resolution of very small structural variations.

In the present work we studied the thermal evolution of the crystal structure and unit-cell parameters of the low-density form of $NaGaSi_2O_6$ [Ga(β) pyroxene; the sample comes from the same batch of synthesis as previously studied by Ohashi et al. 1995] down to 110 K, to verify possible changes in the crystal structure at low temperatures. The study was performed with single-crystal X-ray diffraction methods using a rotating anode, which provides diffraction intensities up to ten times greater than those obtained with a conventional anode. The flexibility of the pyroxene silicate chain makes it possible to observe significant structural differences, even when the temperature range is small as in low-temperature investigations.

EXPERIMENTAL METHODS

The crystal was synthesized by solid-state reaction using a belt-type high-pressure apparatus (as in Ohashi et al. 1995). Mixtures of crystalline $Na_2Si_2O_5$, Ga_2O_3, and SiO_2 were sealed in platinum capsule and maintained at 1770 K and 6 GPa for 5 h. A crystal of size $120 \times 80 \times 70$ μm^3 was chosen for the low-temperature X-ray diffraction measurements. It showed sharp optical extinction and was tested on a Huber four-circle diffractometer (non-monochromatic Mo$K\alpha$ radiation) using the eight-position method of centering for 20 Bragg reflections according to the procedure of King and Finger (1979). No evidence of twinning was found. Centering procedure and vector-least-square refinement of the unit-cell parameters were performed by SINGLE04 software according to Ralph and Finger (1982) and Angel et al. (2000). The unit-cell parameters at room temperature were: a = 9.5551(2) Å, b = 8.7007(3) Å, c = 5.2694(2) Å, β = 107.626(2)°, V = 417.51(2) Å^3. X-ray diffraction at low temperatures was measured on a Nonius Mach3 diffractometer, equipped with a rotating anode using Mo$K\alpha$ radiation (λ = 0.71069 Å). Unit-cell parameters were measured by centering 25 Bragg reflections within the range $43 < 2\theta < 60°$ in four settings (SET4 procedure; Enraf-Nonius 1989). The unit-cell parameters at room temperature are in good agreement with those determined on the Huber diffractometer, in spite of the different experimental procedures [a = 9.5531(3) Å, b = 8.6983(2) Å, c = 5.2684(1) Å, β = 107.629(2)°, and V = 417.22(2) Å^3 for the MACH3 instrument].

Five complete intensity data collections were performed on the Nonius Mach3 diffractometer, at 295, 235, 190, 145, and 110 K, using ω-2θ scans with a scan velocity between 1.3° and 4°/min up to $2\theta_{max} = 80°$. All intensity data were collected on the *C*-centered lattice, after checking for the presence of the *C*-centering down to 110 K (this monitoring was necessary because on the isostructural compound $NaTiSi_2O_6$ a phase transition to triclinic occurs at 197 K, Redhammer et al. 2003). Data reduction was performed using HELENA software (Spek 1997). Absorption correction was performed by HABITUS software (Herrendorf and Bärnighausen 1997), resulting in a strong improvement of the R_{int}. Structure refinements on F^2 were performed using SHELXL97 (Sheldrick 1997). X-ray scattering factors in their neutral form were taken from *International Table of Crystallography* (Wilson 1995). The crystal used for the low-temperature diffraction measurements was subsequently analyzed by electron microprobe using a fully automated four-spectrometer CAMECA SX-50 (acceleration voltage 15 kV; beam currents of 10–15 nA; focused electron beam of approximately 2 μm; internal correction routines of the instrument were used for data reduction and evaluation of elemental concentrations). The following compounds were used as standards: Si, Mg:$MgSiO_3$; Na:$NaAlSi_3O_8$; Ga:GaAs. The chemical formula based on an average of 15 point analyses confirmed the stoichiometric composition: $Na_{1.00(1)}Ga_{1.01(1)}Si_{2.01(1)}O_6$.

RESULTS

Thermal expansion

The unit-cell parameters have been determined at 14 selected temperatures from 295 down to 110 K (Table 1). Both the unit-cell parameters a, b, c, and the volume V of the unit cell decrease down to 110 K in a non-linear way, whereas the angle β remains constant at 107.63° within one standard deviation throughout the investigated range of temperatures Unit-cell parameters exhibit a smooth dependence on temperature, and evidence for a possible structural phase transition is not found in these data (Fig. 2). Mean linear thermal expansion coefficients can be calculated as $\alpha_X(T) = (1/X_{295})[(X_T - X_{295})/(T - 295)]$, where X represents an unit-cell parameter and T is the temperature (Cameron et al. 1973). For T = 110 K they are: $\alpha_a(T) = 5.036(1) \times 10^{-6}$ K^{-1}, $\alpha_b(T) = 8.327(1) \times 10^{-6}$ K^{-1}, $\alpha_c(T) = 2.257(1) \times 10^{-6}$ K^{-1}. The mean thermal expansion coefficient for this temperature range is $\alpha_V(T) = 1.568(1) \times 10^{-5}$ K^{-1}. Thermal expansion is highly anisotropic, with $\alpha_a:\alpha_b:\alpha_c$ = 2.23:3.69:1.

A suitable physical model for the thermal expansion of $NaGaSi_2O_6$ at low temperatures is provided by the Debye model for the density of states of phonons, resulting in the following relation between V and T (Suzuki et al. 1979):

$$V(T) = \frac{V_0}{2k}\left[1 + 2k - \left(1 - 4kE/Q_0\right)^{1/2}\right] \quad (1)$$

where E is the energy of the lattice vibrations, k is a constant, Q_0 is related to the volume (V_0) and bulk modulus (K_{T0}) at zero Kelvin and to the Grüneisen parameter (γ) by $Q_0 = K_0V_0/\gamma$. The

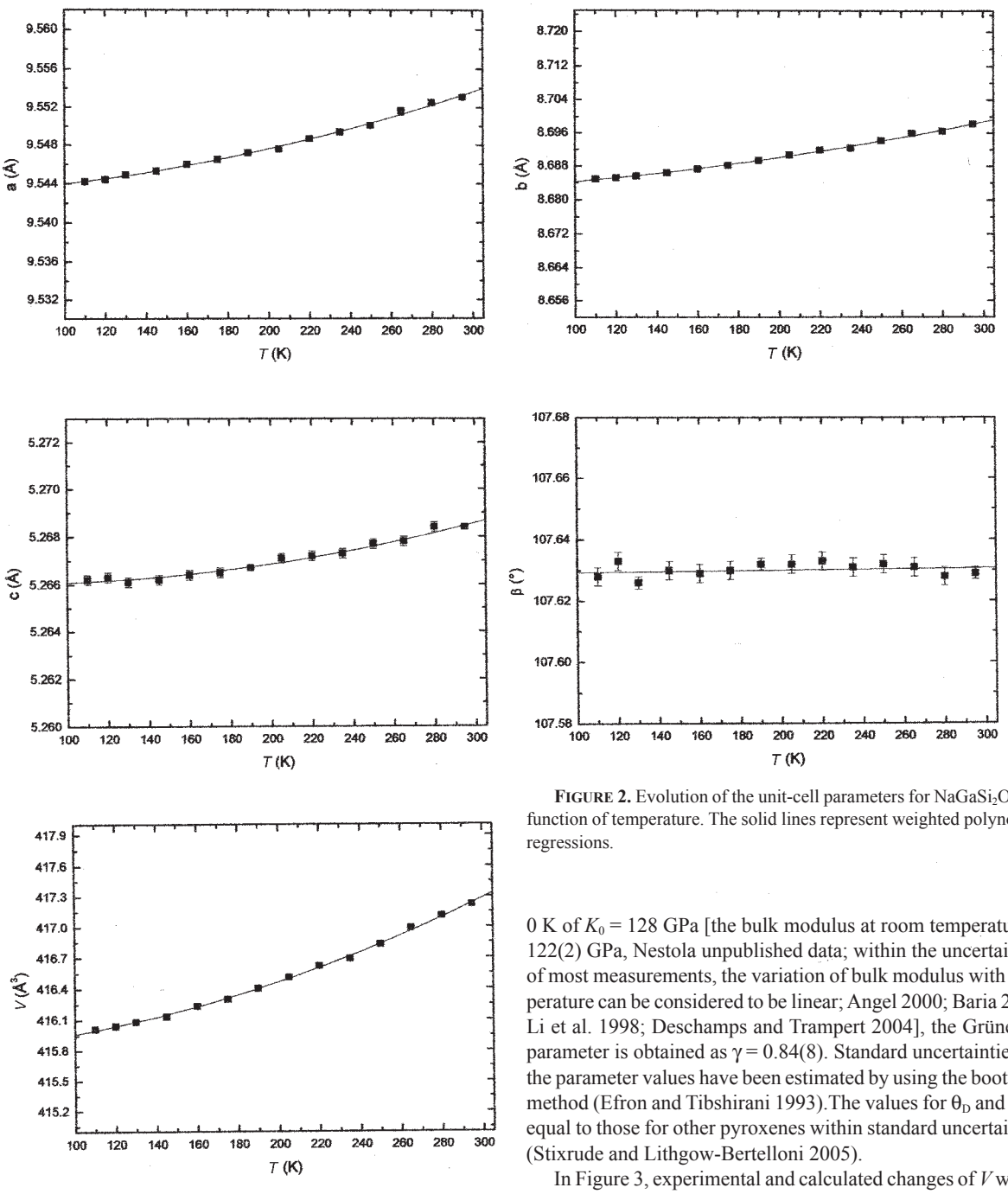

FIGURE 2. Evolution of the unit-cell parameters for $NaGaSi_2O_6$ as a function of temperature. The solid lines represent weighted polynomial regressions.

energy E is calculated from the Debye model (e.g., Fei 1995; Kittel 1966):

$$E = \frac{9nRT}{\left(\theta_D/T\right)^3}\int_0^{\theta_D/T}\frac{x^3}{e^x-1}dx \quad (2)$$

where n, R, and θ_D are the number of atoms in the chemical formula, the gas constant, and the Debye temperature, respectively.

The parameters obtained from a fit of Equation 1 to the data are: V_0 = 415.91(5) Å^3, k = 8(4), Q_0 = 9575(1149) kJ, and θ_D = 653(39) K. Furthermore, with an extrapolated bulk modulus at 0 K of K_0 = 128 GPa [the bulk modulus at room temperature is 122(2) GPa, Nestola unpublished data; within the uncertainties of most measurements, the variation of bulk modulus with temperature can be considered to be linear; Angel 2000; Baria 2004; Li et al. 1998; Deschamps and Trampert 2004], the Grüneisen parameter is obtained as γ = 0.84(8). Standard uncertainties for the parameter values have been estimated by using the bootstrap method (Efron and Tibshirani 1993).The values for θ_D and γ are equal to those for other pyroxenes within standard uncertainties (Stixrude and Lithgow-Bertelloni 2005).

In Figure 3, experimental and calculated changes of V with T are shown. The non-linear behavior at low T is well described, without systematic differences between the data and the model. The goodness of the fit excludes the possible presence of a phase transition. The thermal expansion coefficient as a function of T, α_V, is obtained by differentiating Equation 1 with respect to T, $\alpha_V = 1/V\,(\partial V/\partial T)_P$, and it is reported in Figure 4 (at 295 K, α_V = 2.180(1) × 10^{-5} K^{-1}).

The isochoric heat capacity, C_V, which was calculated as a function of T/θ_D (obtained by deriving Equation 2 with respect to T, $C_V = (\partial V/\partial T)_V$, e.g., Kittel 1966) is reported in Figure 5. C_V is related to the isobaric heat capacity, C_P, by the equation C_P

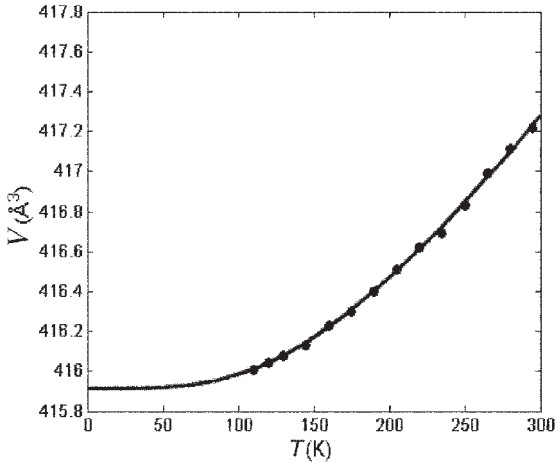

FIGURE 3. Experimental and calculated evolution of unit-cell volume with temperature for $NaGaSi_2O_6$.

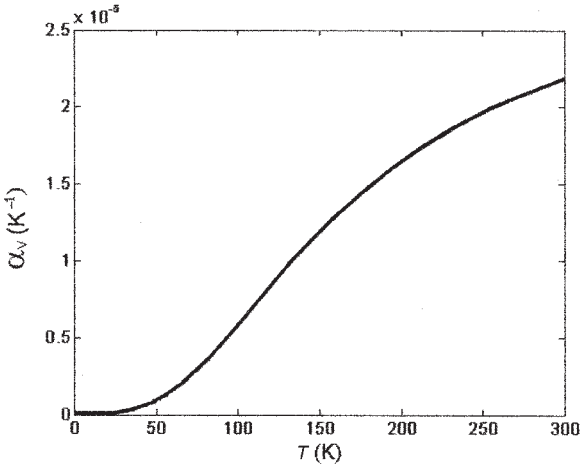

FIGURE 4. Thermal expansion coefficient, α_V, as a function of temperature for $NaGaSi_2O_6$. The curve displayed is a calculated curve according to a differentiation of Equation 1.

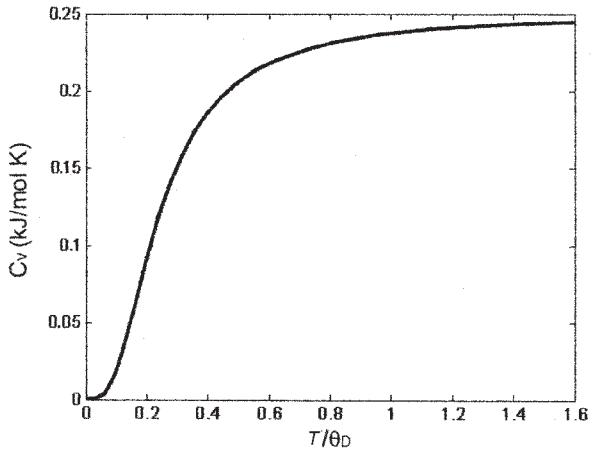

FIGURE 5. Isochoric heat capacity, C_V, as a function of T/θ_D for $NaGaSi_2O_6$.

TABLE 1. Unit-cell parameters of $NaGaSi_2O_6$ at different temperatures

Temperature (K)	*a* (Å)	*b* (Å)	*c* (Å)	β (°)	*V* (Å³)
295	9.5531(3)	8.6983(2)	5.2684(1)	107.629(2)	417.22(2)
280	9.5525(3)	8.6965(2)	5.2684(2)	107.628(3)	417.11(2)
265	9.5516(4)	8.6960(2)	5.2678(2)	107.631(3)	416.99(2)
250	9.5501(3)	8.6942(2)	5.2677(2)	107.632(3)	416.83(2)
235	9.5494(3)	8.6924(2)	5.2673(2)	107.631(3)	416.69(2)
220	9.5487(3)	8.6919(2)	5.2672(2)	107.633(3)	416.62(2)
205	9.5476(3)	8.6907(2)	5.2671(2)	107.632(3)	416.51(2)
190	9.5472(3)	8.6894(2)	5.2667(1)	107.632(2)	416.40(2)
175	9.5465(3)	8.6882(2)	5.2665(2)	107.630(3)	416.30(2)
160	9.5460(3)	8.6873(2)	5.2664(2)	107.629(3)	416.23(2)
145	9.5453(3)	8.6864(2)	5.2662(2)	107.630(3)	416.13(2)
130	9.5449(3)	8.6856(2)	5.2661(2)	107.626(2)	416.08(2)
120	9.5444(3)	8.6852(2)	5.2663(2)	107.633(3)	416.04(2)
110	9.5442(3)	8.6849(2)	5.2662(2)	107.628(3)	416.01(2)

Note: One standard deviation is reported in parentheses.

$- C_V = T\alpha^2_V V_m K_T$, where V_m is the molar volume and K_T is the bulk modulus. The difference between C_P and C_V is relatively small and can be neglected, in particular below room temperature (given that $\alpha_V = 2.18 \times 10^{-5}$ K^{-1}, $V_m = 6.28$ kJ/kbar (≈417 Å^3), $T =$ 298 K, and $K_T = 1220$ kbar, $(C_P - C_V)$ is $\approx 1 \times 10^{-3}$ kJ/mol·K.).

Temperature dependence of the crystal structure

Complete intensity data collections were carried out at five different temperatures: 295, 235, 190, 145, and 110 K. Structure refinements were performed, starting with the atomic coordinates of Ohashi et al. (1995). They confirmed the space group to be *C*2/*c* down to 110 K. All the refinement and crystal data are reported in Table 2, whereas the refinement results (atomic fractional coordinates, displacement parameters, bond distances, angles, and polyhedral data) are reported in Tables 3 and 4.

M2 site

The polyhedral volume of M2, M1, and T sites and their standard deviations were calculated using IVTON software (Balic-Zunic et al. 1996). The M2 volume at room temperature is 25.442(15) Å^3 (Table 4) and shows a linear trend down to 110 K without discontinuities (Fig. 6a). It shrinks by 0.50% down to 110 K. As observed in general for clinopyroxenes, this polyhedron undergoes the strongest variations under non-ambient conditions. All the Na-O bond lengths in the irregular M2 polyhedron decrease with decreasing temperature (Table 4). The average bond length <Na-O> decreases linearly without discontinuities (Fig. 7a). The largest decrease is shown by the Na-O3(C2,D2) distances (the nomenclature used in this work is taken from Clark et al. 1969) with a variation of 0.29%, while the smallest decrease is for the Na-O3(C1; D1) distances, with a change of 0.11% with respect to the room temperature value (Figs. 8a and 8b). Na-O3(C1,D1), Na-O2(C2,D2), and Na-O3(C1,D1) bond distances do not show discontinuities in their temperature dependencies (Figs. 8a–8c), while the Na-O1(A1,B1) distances exhibit anomalies between 145 and 190 K (Fig. 8d).

M1 site

The octahedral volume of the M1 site is 10.289(6) Å^3 at room temperature and decreases by 0.30% down to 110 K (Table 4). It shows an anomaly between 235 and 190 K, while it becomes independent of temperature at lower temperatures (Fig. 6b). The <Ga-O> average bond distance exhibits an anomaly within the

TABLE 2. Experimental crystal-structure details concerning the data collections and the structure refinements at different temperatures for $NaGaSi_2O_6$

	295 K	235 K	190 K	145 K	110 K
Crystal data					
Chemical formula	$NaGaSi_2O_6$	$NaGaSi_2O_6$	$NaGaSi_2O_6$	$NaGaSi_2O_6$	$NaGaSi_2O_6$
M_r	244.88	244.88	244.88	244.88	244.88
a (Å)	9.5531(3)	9.5494(3)	9.5472(3)	9.5453(3)	9.5442(3)
b (Å)	8.6983(2)	8.6924(2)	8.6894(2)	8.6864(2)	8.6849(2)
c (Å)	5.2684(1)	5.2673(2)	5.2667(1)	5.2662(2)	5.2662(2)
β (°)	107.629(2)	107.631(3)	107.632(2)	107.630(3)	107.628(3)
V (Å^3)	417.22(2)	416.69(2)	416.40(2)	416.13(2)	416.01(2)
S.G.	*C*2/*c*	*C*2/*c*	*C*2/*c*	*C*2/*c*	*C*2/*c*
Z	4	4	4	4	4
D_x (Mg m^{-3})	3.899	3.904	3.906	3.909	3.910
Radiation type	Mo*K*α	Mo*K*α	Mo*K*α	Mo*K*α	Mo*K*α
No. refl. for the unit cell parameters	25	25	25	25	25
θ range for the unit cell parameters (°)	21.5–30	21.5–30	21.5–30	21.5–30	21.5–30
μ (mm^{-1})	7.22	7.23	7.23	7.24	7.24
Crystal form, color	Prismatic, light brown	Prismatic, light brown	Prismatic, light brown	Prismatic, light brown	Prismatic, light brown
Crystal size (mm)	0.120 × 0.08 × 0.07	0.120 × 0.08 × 0.07	0.120 × 0.08 × 0.07	0.120 × 0.08 × 0.07	0.120 × 0.08 × 0.07
Data collection					
Diffractometer	Nonius Mach3 (rotating anode)	Nonius Mach3 (rotating anode)	Nonius Mach3 (rotating anode)	Nonius Mach3 (rotating anode)	Nonius Mach3 (rotating anode)
Data coll. method	ω-2θ scan	ω-2θ scan	ω-2θ scan	ω-2θ scan	ω-2θ scan
Absorption correction	Habitus software	Habitus software	Habitus software	Habitus software	Habitus software
T_{min}	0.5348	0.5351	0.5355	0.5359	0.5362
T_{max}	0.7071	0.7071	0.7071	0.7071	0.7072
Range of *h*, *k*, *l*	$-17 \le h \le 16$ $-15 \le k \le 15$ $0 \le l \le 9$	$-17 \le h \le 16$ $-15 \le k \le 15$ $0 \le l \le 9$	$-17 \le h \le 16$ $-15 \le k \le 15$ $0 \le l \le 9$	$-17 \le h \le 16$ $-15 \le k \le 15$ $0 \le l \le 9$	$-17 \le h \le 16$ $-15 \le k \le 15$ $0 \le l \le 9$
No. of measured, independent and observed reflections	2779, 1291, 1186	2779, 1291, 1194	2778, 1291, 1195	2778, 1291, 1193	2777, 1291, 1196
Criterion for observed reflections	$I > 4\sigma$	$I > 4\sigma$	$I > 4\sigma$	$I > 4\sigma$	$I > 4\sigma$
R_{int}	0.020	0.017	0.016	0.018	0.016
θ_{max} (°)	39.96	39.94	39.95	39.96	39.96
Refinement					
Refinement on *R* [$F^2 > 4\sigma(F^2)$], w*R*(F^2), S	0.0166, 0.046, 1.14	0.0156, 0.040, 0.99	0.0149, 0.043, 1.14	0.0154, 0.044, 1.15	0.0149, 0.042, 1.14
No. reflections	1186	1194	1195	1193	1196
No. parameters	48	48	48	48	48
Weighting scheme	$1/[\sigma^2(Fo^2) + 0.0216P)^2]$	$1/[\sigma^2(Fo^2) + (0.0125P)^2 + P]$	$1/[\sigma^2(Fo^2) + (0.0171P)^2 + 0.27P]$	$1/[\sigma^2(Fo^2) + (0.0178P)^2 + 0.19P]$	$1/[\sigma^2(Fo^2) + (0.0171P)^2 + 0.27P]$
$P = (F_o^2 + F_c^2)/3$					
$(\Delta/\sigma)_{max}$	<0.0001	<0.0001	<0.0001	<0.0001	<0.0001
$\Delta\rho_{max}$, $\Delta\rho_{min}$ (e Å^{-3})	0.59, –0.84	0.51, –0.47	0.48, –0.54	0.55, –0.48	0.46, –0.47
Extinction method	*SHELXL*	*SHELXL*	*SHELXL*	*SHELXL*	*SHELXL*
Extinction coefficient	0.0136	0.0124	0.0120	0.0128	0.0122

same range of temperatures (Fig. 7b). The largest variation for the Ga-O bond distances is shown by Ga-O1(A1,B1) (Fig. 9a) with a smooth decrease of up to 0.24% at 110K. Ga-O1(A2,B2) and Ga-O2(C1,D1) bond distances have small variations of 0.02% and 0.06%, respectively (Table 4), but they exhibit anomalies in their temperature dependencies (Figs. 9b and 9c). The three independent bond angles of the M1 octahedron, O1(A1,B1)-Ga-O1(A2,B2), O1(A1,B1)-Ga-O2(C1,D1), and O1(A2,B2)-Ga-O2(C1,D1), also exhibit anomalous behavior (Fig. 10), which gives an indication of the octahedral distortion.

T site

The tetrahedral polyhedron T for clinopyroxenes is considered a rigid unit showing always very small values of compressibilities and thermal expansion coefficients (Zhang et al. 1997; Angel and Hugh-Jones 1994; Nestola et al. 2004). This site is occupied by Si (Fig. 1) and has a volume of 2.197(2) Å^3 at room temperature. As expected, its variation from room temperature down to 110 K is smaller than one standard deviation (Fig. 11a). The <Si-O> average bond distance does not show appreciable variations with temperature. The only Si-O bond distance, showing a variation larger than one standard deviation, is the Si-O3A1 (Fig. 11b) with a very small non-linear expansion (about 0.10%). The evolution with temperature of the O3-O3-O3 angle, that defines the kinking of the tetrahedral silicate chain of the clinopyroxenes along **c**, shows a small but non-linear decrease on decreasing temperature, from 172.77(6)° at room temperature to 172.50(6)° at 110 K.

DISCUSSION

Thermal expansion

Anisotropic thermal expansion of Na pyroxenes is not completely characterized by the three linear expansion coefficients, because the angle β of the monoclinic lattice may also depend on temperature. Instead, the deformation has to be calculated from the unit-cell parameters at low and high temperatures, which can be described by the sizes and orientations of strain ellipsoids. The strain ellipsoid was calculated for $NaGaSi_2O_6$ using the software STRAIN (Ohashi 1982) from cell parameters at the highest and lowest temperatures (298 and 110 K), and by comparing cell parameters at ΔT intervals of about 60 K. The results are shown

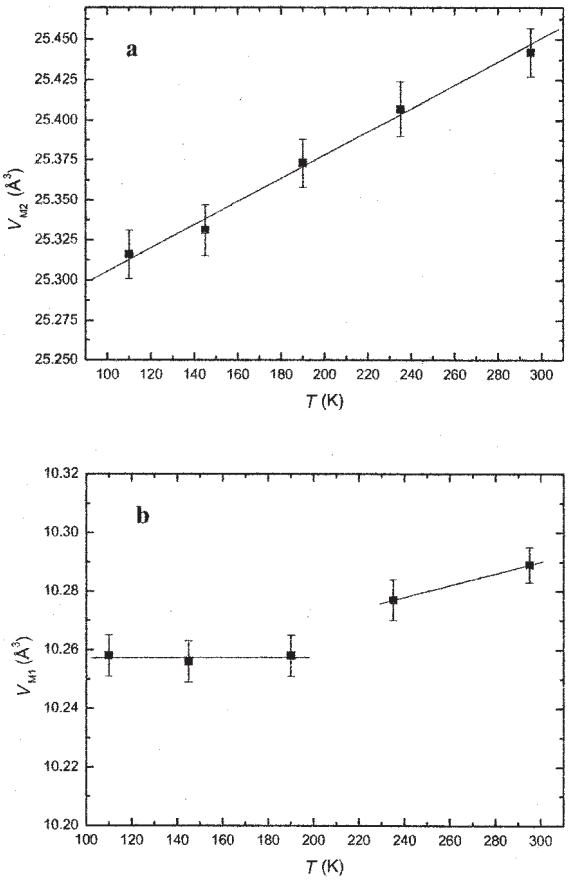

FIGURE 6. Polyhedral volume evolution as a function of temperature for the M2 polyhedron (**a**) and M1 octahedron (**b**) of $NaGaSi_2O_6$. The volumes and their standard deviations have been calculated using IVTON software (Balic-Zunic and Vickovic 1996).

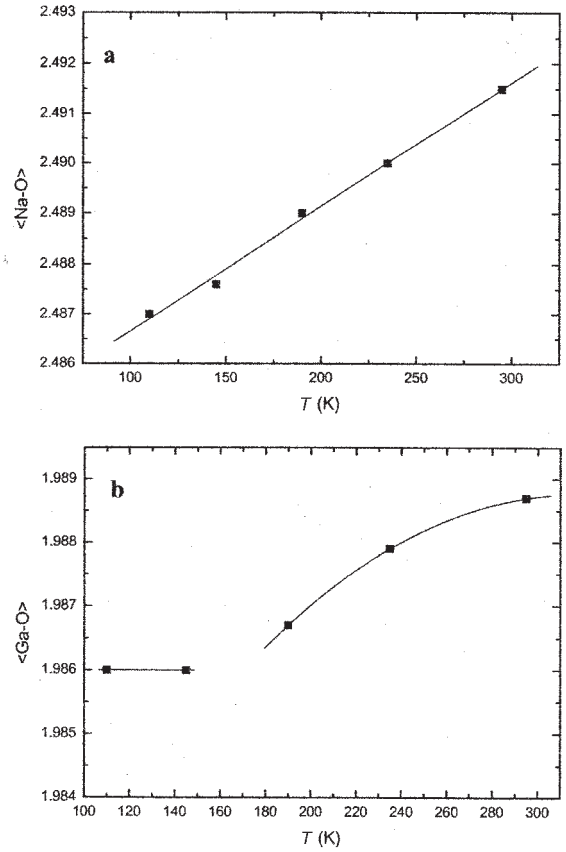

FIGURE 7. Evolution of Na-O (**a**) and Ga-O (**b**) average bond distances with temperature for $NaGaSi_2O_6$.

in Table 5. The first principal axis lies along the monoclinic axis (**b** axis), and the orientation of the other two axes is similar for the different intervals. The deformation scheme is qualitatively the same as in other pyroxenes, with the largest deformation along the **b** axis. The orientations of the principal axes of the strain ellipsoid in the (010) plane vary with temperature. One principal axis is oriented about 100° from the **c** axis, as is also found in jadeite ($NaAlSi_2O_6$). In kosmochlor ($NaCrSi_2O_6$) and aegirine ($NaFe^{3+}Si_2O_6$), this principal axis is located at 68° and 75°, respectively, from the **c** axis. (Table 5). This difference is probably related to the electronic structure of the M1 cation: in kosmochlor and aegirine M is a transition metal, whereas in the others it is not.

In summary, $NaGaSi_2O_6$ behaves similarly to other Na pyroxenes as far as the temperature dependences of the unit-cell parameters and the Debye temperature and the Grüneisen parameter are concerned.

Bonding behavior of $NaGaSi_2O_6$ at low temperature

We have investigated a sample of the low-density form $NaGa(\beta)Si_2O_6$ that has been suggested to be different than the high-density form $NaGa(\alpha)Si_2O_6$ (Ohashi et al. 1983, 1995). The unit-cell parameters do not show any discontinuity in the

TABLE 3. Atomic fractional coordinates, equivalent isotropic, and anisotropic displacement parameters (Å^2) at different temperatures for $NaGaSi_2O_6$

		295 K	235 K	190 K	145 K	110 K
Na	*x*	0.00000	0.00000	0.00000	0.00000	0.00000
	y	0.30038(7)	0.30046(8)	0.30051(7)	0.30047(7)	0.30058(7)
	z	0.25000	0.25000	0.25000	0.25000	0.25000
	U_{eq}	0.0108(1)	0.0090(1)	0.0074(1)	0.0062(1)	0.0052(1)
Ga	*x*	0.00000	0.00000	0.00000	0.00000	0.00000
	y	0.90189(1)	0.90210(2)	0.90219(2)	0.90232(2)	0.90238(2)
	z	0.25000	0.25000	0.25000	0.25000	0.25000
	U_{eq}	0.00348(5)	0.00294(4)	0.00244(4)	0.00201(4)	0.00163(4)
Si	*x*	0.29116(3)	0.29119(3)	0.29119(3)	0.29121(3)	0.29125(3)
	y	0.09112(3)	0.09122(3)	0.09127(3)	0.09129(3)	0.09128(3)
	z	0.23220(5)	0.23236(5)	0.23241(5)	0.23263(5)	0.23264(5)
	U_{eq}	0.00314(5)	0.00274(5)	0.00237(5)	0.00206(5)	0.00183(5)
O1	*x*	0.11188(7)	0.11199(8)	0.11191(8)	0.11187(8)	0.11190(8)
	y	0.07804(7)	0.07797(8)	0.07803(7)	0.07812(8)	0.07820(7)
	z	0.13365(14)	0.13373(14)	0.13350(14)	0.13369(14)	0.13385(14)
	U_{eq}	0.0044(1)	0.0037(1)	0.0032(1)	0.0030(1)	0.00276(9)
O2	*x*	0.35874(8)	0.35868(8)	0.35878(8)	0.35880(8)	0.35882(8)
	y	0.25894(8)	0.25913(8)	0.25935(8)	0.25936(8)	0.25945(8)
	z	0.30170(14)	0.30187(15)	0.30219(14)	0.30240(14)	0.30267(14)
	U_{eq}	0.0062(1)	0.0053(1)	0.0046(1)	0.0039(1)	0.0034(1)
O3	*x*	0.35265(7)	0.35284(8)	0.35285(7)	0.35303(7)	0.35297(7)
	y	0.00957(9)	0.00984(9)	0.00980(8)	0.00986(8)	0.00994(8)
	z	1.00787(13)	1.00773(15)	1.00769(13)	1.00795(13)	1.00775(13)
	U_{eq}	0.0055(1)	0.0048(1)	0.0041(1)	0.0036(1)	0.0032(1)

Note: One standard deviation is reported in parentheses.

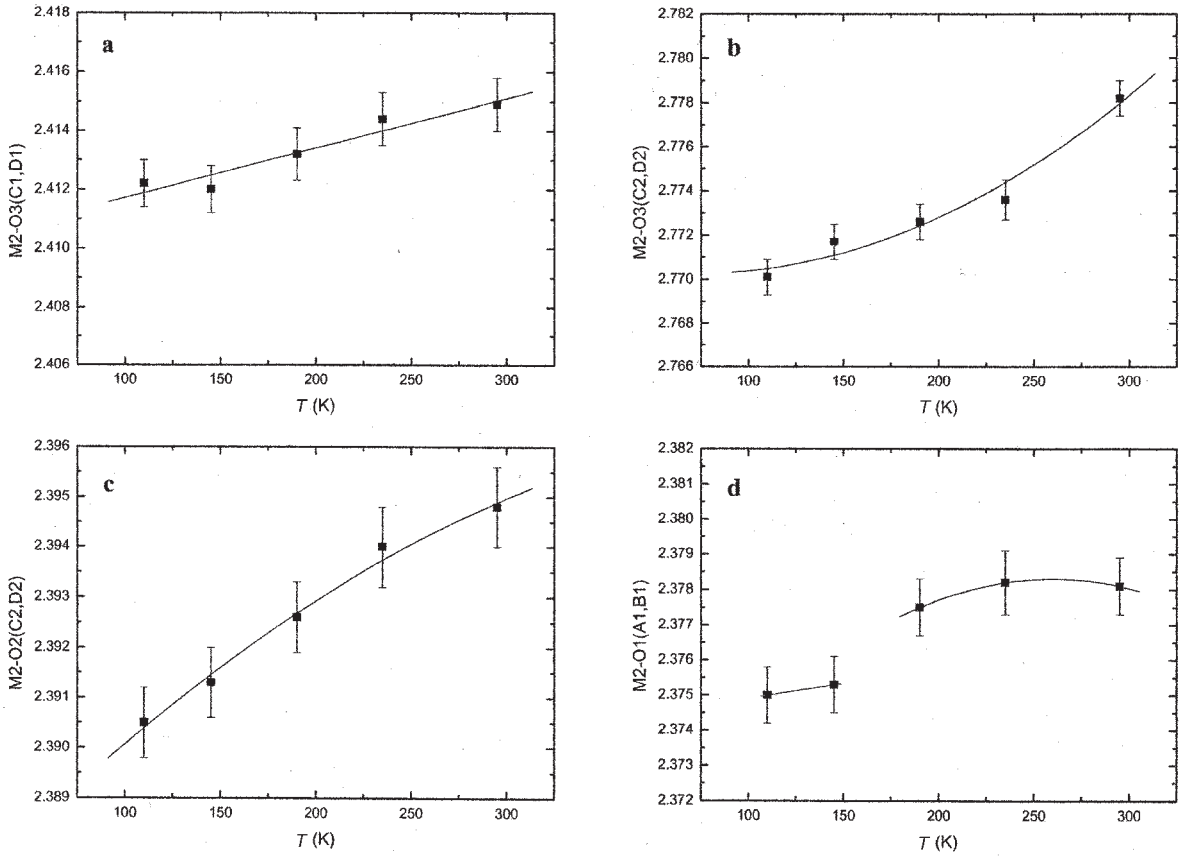

FIGURE 8. Bond distances evolution as a function of temperature for the M2 polyhedron: (**a**) Na-O3(C1,D1); (**b**) Na-O3(C2,D2); (**c**) Na-O2(C2,D2); (**d**) Na-O1(A1,B1).

TABLE 4. Selected bond lengths (Å), bond angles (°), and polyhedral volumes at different temperatures for $NaGaSi_2O_6$

Temperatures (K)	295	235	190	145	110
M2 polyhedron					
Na-O1(A1,B1)×2 (Å)	2.3781(8)	2.3782(9)	2.3775(8)	2.3753(8)	2.3750(8)
Na-O2(C2,D2)×2 (Å)	2.3948(8)	2.3940(8)	2.3926(7)	2.3913(7)	2.3905(7)
Na-O3(C1,D1)×2 (Å)	2.4149(9)	2.4144(9)	2.4132(9)	2.4120(8)	2.4122(8)
Na-O3(C2,D2)×2 (Å)	2.7782(8)	2.7736(9)	2.7726(8)	2.7717(8)	2.7701(8)
<Na-O> (Å)	2.492(2)	2.490(2)	2.489(2)	2.488(2)	2.487(2)
V_{M2} (Å^3)	25.442(15)	25.407(17)	25.373(15)	25.331(16)	25.316(15)
M1 octahedron					
Ga-O1(A1,B1)×2 (Å)	2.0646(7)	2.0622(7)	2.0615(7)	2.0600(7)	2.0596(7)
Ga-O1(A2,B2)×2 (Å)	1.9874(7)	1.9874(7)	1.9858(7)	1.9862(7)	1.9869(7)
Ga-O2(C1,D1)×2 (Å)	1.9142(7)	1.9141(7)	1.9127(7)	1.9131(7)	1.9131(7)
<Ga-O> (Å)	1.989(2)	1.988(2)	1.987(2)	1.986(2)	1.986(2)
V_{M1} (Å^3)	10.289(6)	10.277(7)	10.258(7)	10.256(7)	10.258(7)
*OAV	43.387	43.069	43.155	42.858	42.646
O1(A1,B1)-Ga-O1(A2,B2)(°)	93.98(3)	94.00(3)	94.06(3)	94.11(3)	94.12(3)
O1(A1,B1)-Ga-O2(C1,D1) (°)	89.38(3)	89.28(3)	89.24(3)	89.26(3)	89.24(3)
O1(A2,B2)-Ga-O2(C1,D1) (°)	90.95(3)	90.93(3)	90.96(3)	90.98(3)	91.00(3)
T tetrahedron					
Si-O1 (Å)	1.6362(7)	1.6349(8)	1.6352(7)	1.6354(7)	1.6353(7)
Si-O2 (Å)	1.5933(7)	1.5927(8)	1.5940(7)	1.5934(7)	1.5940(7)
Si-O3A1 (Å)	1.6327(7)	1.6336(8)	1.6342(7)	1.6344(7)	1.6344(7)
Si-O3A2 (Å)	1.6446(7)	1.6446(8)	1.6440(7)	1.6444(7)	1.6437(7)
<Si-O> (Å)	1.627(1)	1.626(1)	1.627(1)	1.627(1)	1.627(1)
V_T (Å^3)	2.197(2)	2.197(2)	2.198(2)	2.198(2)	2.198(2)
Kinking of tetrahedral chain O3-O3-O3 (°)	172.77(6)	172.60(6)	172.55(6)	172.64(6)	172.50(6)

Note: In parentheses, one standard deviation is reported.
* Octahedral angle variance as in Robinson et al. (1971).

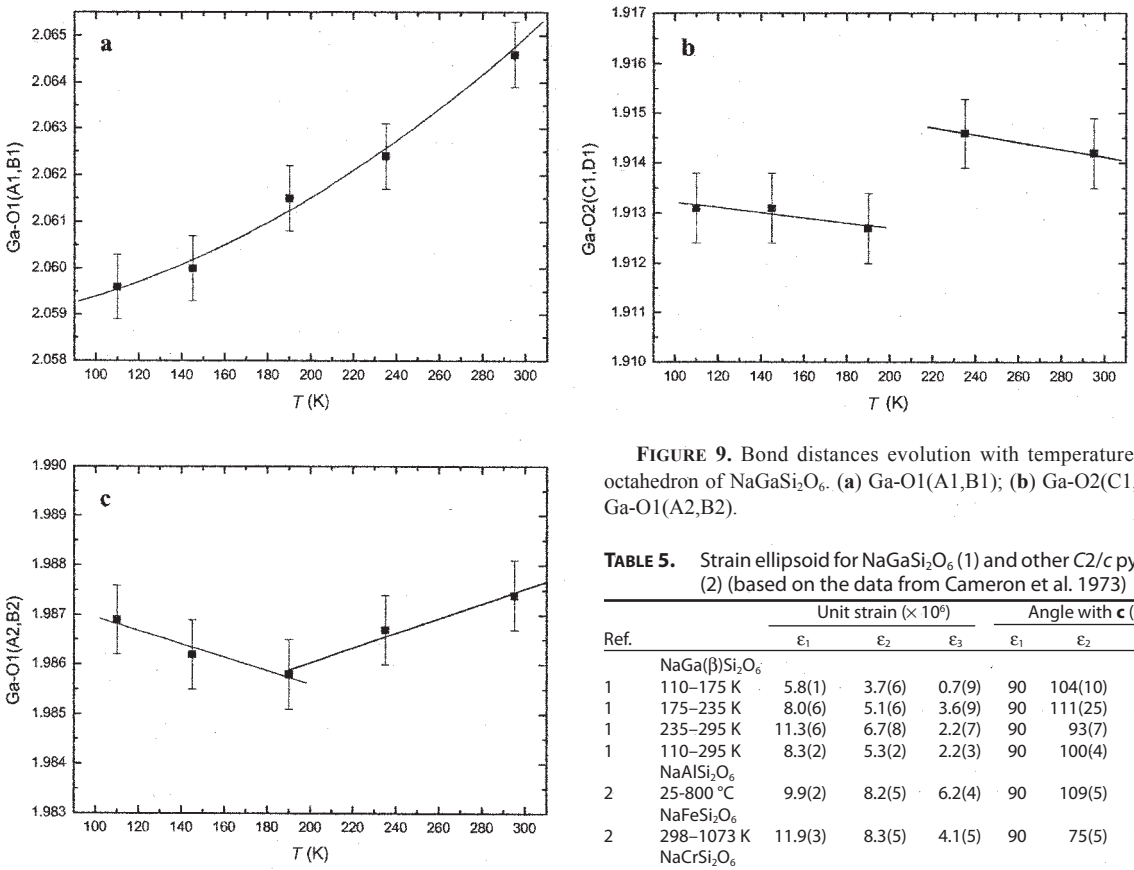

FIGURE 9. Bond distances evolution with temperature for M2 octahedron of $NaGaSi_2O_6$. (**a**) Ga-O1(A1,B1); (**b**) Ga-O2(C1,D1); (**c**) Ga-O1(A2,B2).

TABLE 5. Strain ellipsoid for $NaGaSi_2O_6$ (1) and other *C*2/*c* pyroxenes (2) (based on the data from Cameron et al. 1973)

		Unit strain (× 10^6)			Angle with **c** (°)		
Ref.		ε_1	ε_2	ε_3	ε_1	ε_2	ε_3
	$NaGa(\beta)Si_2O_6$						
1	110–175 K	5.8(1)	3.7(6)	0.7(9)	90	104(10)	14(10)
1	175–235 K	8.0(6)	5.1(6)	3.6(9)	90	111(25)	22(25)
1	235–295 K	11.3(6)	6.7(8)	2.2(7)	90	93(7)	3(7)
1	110–295 K	8.3(2)	5.3(2)	2.2(3)	90	100(4)	10(4)
	$NaAlSi_2O_6$						
2	25-800 °C	9.9(2)	8.2(5)	6.2(4)	90	109(5)	19(5)
	$NaFeSi_2O_6$						
2	298–1073 K	11.9(3)	8.3(5)	4.1(5)	90	75(5)	−15(5)
	$NaCrSi_2O_6$						
2	298–873 K	9.6(3)	7.7(4)	3.4(4)	90	68(4)	−22(4)

investigated range of temperatures and no evidence of a structural phase transition was found.

As a first result, $NaGaSi_2O_6$ does not show the *C*2/*c*-$P\bar{1}$ phase transition found in the isostructural $NaTiSi_2O_6$ at 200 K (Redhammer et al. 2003). This would indicate that the substitution of a smaller cation as Ga for Ti at the M1 site (ionic radii are 0.67 Å for Ti and 0.62 Å for Ga, Shannon 1976) would stabilize the higher symmetry phase, increasing the stability field of the *C*2/*c* space group toward lower temperatures. However, $NaFeSi_2O_6$ pyroxene, which has a M1 cation radius very close to that of $NaTiSi_2O_6$ (Fe^{3+} = 0.645 Å, Shannon 1976), does not show any symmetry change down to 30 K (Redhammer and Roth 2002), assuming that the monoclinic-triclinic phase transition for Na clinopyroxenes is related to the M1 cation radius. Also for Li-bearing clinopyroxenes ($LiM^{3+}Si_2O_6$ with M^{3+} = Cr, Ga, Sc, V, Al, In) a phase transition $P2_1/c$-*C*2/*c* occurs at low temperature but it is not simply related to a change in cationic radius at M1 site, as shown by Redhammer and Roth 2004. These authors suggested that a key role in the transformation is represented by the extension of the tetrahedral chain (O3–O3–O3 angle). Samples with nearly fully extended tetrahedral chains (O3–O3–O3 angle close 180°) at ambient conditions undergo phase transitions at low temperatures, while those with chains more kinked do not show a phase transition. However, for the monoclinic-triclinic phase transition in Na-bearing clinopyroxenes the relation between the change in symmetry and the extension of the tetrahedral chain is not apparent: $NaTiSi_2O_6$ clinopyroxene (Redhammer et al. 2003) with a tetrahedral chain showing a kinking angle of about 174° has a phase transition at about 200 K, whereas $NaFeSi_2O_6$ with an almost identical kinking angle of 174.2° does not show any transformation down to 30 K (Redhammer and Roth 2002). Furthermore, as shown in this study, $NaGaSi_2O_6$ with a kink angle of 172.77° does not show a phase transformation down to 110 K. It can therefore be concluded that possible phase transitions of Na-bearing clinopyroxenes are not related to the radii of the M cations or to the extension of the tetrahedral chain. As suggested by Redhammer et al. (2003), principal differences between pyroxenes are related to the electronic configurations of the M1 cations. Some compounds containing transition elements do show phase transitions, while it seems that compounds without transition elements do not exhibit phase transitions. For pyroxenes containing 3d transition elements at M1 site, the nature of the low-temperature phase transition could be related to the 3d electron shell as shown by Redhammer et al. (2003). Their plot of M1-M1 distances vs. M1-O mean bond distances indicates that pyroxenes with a symmetric 3d electron shell (e.g., $NaFeSi_2O_6$, $NaGaSi_2O_6$, and $NaAlSi_2O_6$) lie on the same linear trend and do not show a low-temperature phase transition. In contrast, pyroxenes with an asymmetrical 3d electron shell (e.g., $NaTiSi_2O_6$) lie outside this trend and undergo a phase transition at

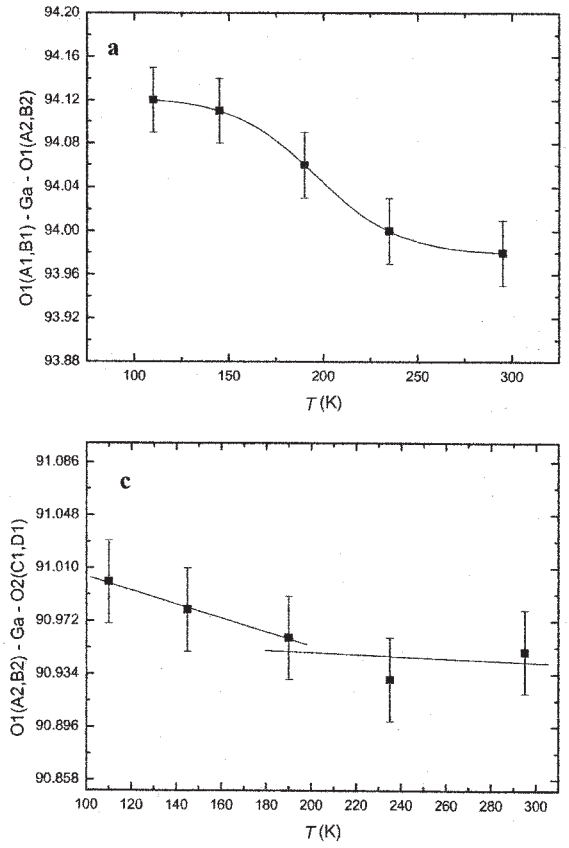

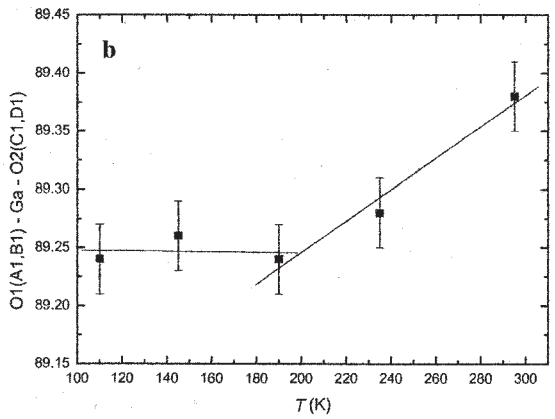

FIGURE 10. Evolution as a function of temperature of the three independent bond angles (**a**) O1(A1,B1)-Ga-O1(A2,B2), (**b**) O1(A1,B1)-Ga-O2(C1,D1), and (**c**) O1(A2,B2)-Ga-O2(C1,D1) for $NaGaSi_2O_6$.

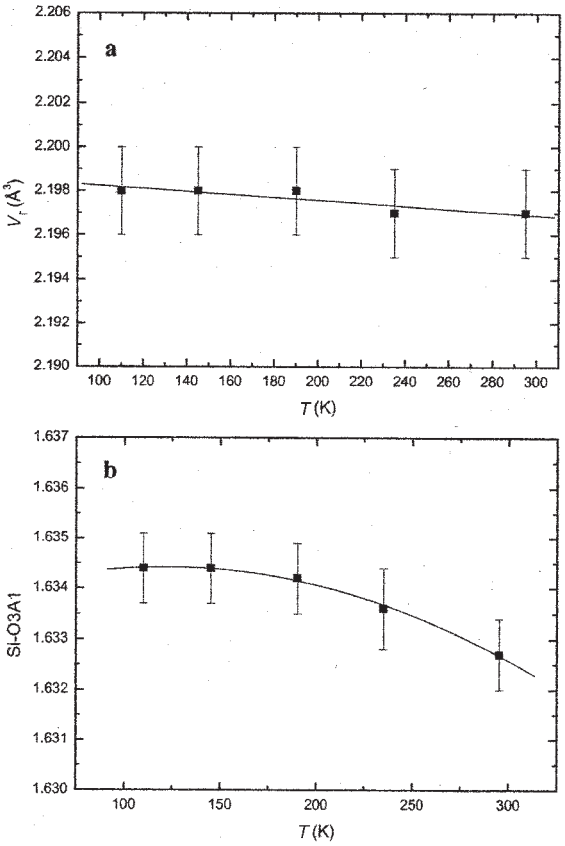

FIGURE 11. Tetrahedral volume evolution as a function of (**a**) temperature and (**b**) variation of Si-O3A1 bond distance down to 110 K for $NaGaSi_2O_6$. The volume and its standard deviation has been calculated using IVTON software (Balic-Zunic and Vickovic 1996).

low temperature. Unfortunately, it is not possible to demonstrate such a hypothesis because there are no data for samples such as $NaCrSi_2O_6$, $NaVSi_2O_6$, and $NaMnSi_2O_6$, which also lie outside the M1-M1 vs. M1-O trend. X-ray diffraction experiments on such samples are in progress at low temperature to verify the presence of low-temperature triclinic symmetry.

Anomalies in their temperature dependencies have presently been found for several structural parameters of $NaGaSi_2O_6$, in particular the volume, bond lengths, and strain deformation of the M1 octahedron (Figs. 6, 9, and 10). The observed anomalies are, however, not related to a transformation from $NaGa(\beta)Si_2O_6$ to $NaGa(\alpha)Si_2O_6$ as proposed by Ohashi et al. (1995) for the following reasons: (1) the average M1-O bond length extrapolated up to room temperature from the two values at lowest temperatures has a value of 1.986 Å; this value is closer to that of $NaGa(\beta)Si_2O_6$ (1.989 Å) than that of $NaGa(\alpha)Si_2O_6$ (1.982 Å) at room temperature. (2) The Ga-O1(A2,B2) bond length is found at all temperatures to be longer than 1.986 Å, which is the value at room temperature for $NaGa(\beta)Si_2O_6$. The corresponding bond length in $NaGa(\alpha)Si_2O_6$ is 1.973 Å. (3) The octahedral angle (Table 4, OAV, Robinson et al. 1971) for the M1 polyhedron shows values between 42.6° (at 110 K) and 43.4° (at 295 K); such values are quite different from the OAV of 46.0° at room temperature in $NaGa(\alpha)Si_2O_6$.

A possible explanation for the discontinuities in the shape of the M1 polyhedron is that of an isostructural rearrangement, involving the Ga-O polyhedral bond distances and angles. Analysis of the electron configuration via an initio Hartree-Fock methods is currently under investigation to clarify this issue.

ACKNOWLEDGMENTS

This project was supported by the Alexander von Humboldt Foundation to Fabrizio Nestola. We thank George Lager, Diego Gatta, Joseph R. Smyth, and

Richard M. Thompson for their very useful reviews. We also thank Detlef Krausse and Anke Potzel for collecting the electron microprobe data and Hubert Schulze for preparing thin sections from single-crystal for microprobe analyses.

REFERENCES CITED

Angel, R.J. (2000) Equations of state. In R.M. Hazen and R.T. Downs, Eds., High-Temperature and High-Pressure Crystal Chemistry, 41, p. 117–221. Reviews in Mineralogy and Geochemistry, Mineralogical Society of America, Chantilly, Virginia.

Angel, R.J. and Hugh-Jones, D.A. (1994) Equation of state and thermodynamic properties of enstatie pyroxenes. Journal of Geophysical Research, 99, 1977–1983.

Angel, R.J., Downs, R.T., and Finger, L.W. (2000) High-temperature-high-pressure diffractometry. In R.M. Hazen and R.T. Downs, Eds., High-temperature and high-pressure crystal chemistry, 41, p. 559–596. Reviews in Mineralogy and Geochemistry, Mineralogical Society of America, Chantilly, Virginia.

Balic-Zunic, T. and Vickovic, I. (1996) IVTON—program for the calculation of geometrical aspects of crystal structures and some chemical applications. Journal of Applied Crystallography, 29, 305–306.

Baria, J.K. (2004) Temperature dependent lattice mechanical properties of some fcc transition metals. Chinese Journal of Physics, 42, 287–306.

Cameron, M., Sueno, S., Prewitt, C.T., and Papike, J.J. (1973) High-temperature crystal chemistry of acmite, diopside, hedenbergite, jadeite, spodumene, and ureyite. American Mineralogist, 58, 594–618.

Clark, J.R., Appleman, D.E., and Papike, J.J. (1969) Crystal-chemical characterization of clinopyroxenes based on eight new structure refinements. Mineralogical Society of America Special Paper, 2, 31–50.

Deschamps, F. and Trampert, J. (2004) Towards a lower mantle reference temperature and composition. Earth and Planetary Science Letters, 222, 161–175.

Efron, B. and Tibshirani, R.J. (1993) An introduction to the bootstrap. Monographs on statistics and applied probability, 57, p. 456. Chapman and Hall, New York.

Enraf-Nonius (1989) CAD-4 Software. Enraf-Nonius, Delft, The Netherlands.

Fei, Y. (1995) Thermal Expansion. In J.A. Ahrens, Ed., A Handbook of physical constants, mineral physics and crystallography. AGU Reference Shelf, 2, 29–44.

Gatta, G.D., Boffa Ballaran, T., and Iezzi G. (2005) High-pressure X-ray and Raman study of a ferrian magnesian spodumene. Physics and Chemistry of Minerals, 32, 132–139.

Hawthorne, F.C. and Grundy, H.D. (1974) Refinement of crystal structure of $NaInSi_2O_6$. Acta Crystallographica B, 30, 1882–1885.

Herrendorf, W. and Bärnighausen, H. (1997) HABITUS. University of Karlsruhe, Germany.

King, H. and Finger, L.W. (1979) Diffracted beam crystal centering and its application to high-pressure crystallography. Journal of Applied Crystallography, 12, 374–378.

Kittel, C. (1966) Introduction to solid state physics, p. 665. Wiley, New York.

Li, B., Liebermann, R.C., and Weidner, D.J. (1998) Elastic moduli of wadsleyite (β-Mg_2SiO_4) to 7 GPa and 873 Kelvin. Science, 281, 675–677.

Nestola, F., Tribaudino, M., and Boffa Ballaran, T. (2004) High-pressure behavior, transformation and crystal structure of synthetic iron-free pigeonite. American Mineralogist, 89, 189–196.

Nestola, F., Boffa Ballaran, T., Liebske, C., Bruno, M., and Tribaudino, M. (2006) High-pressure behavior along the jadeite $NaAlSi_2O_6$-aegirine $NaFeSi_2O_6$ solid solution up to 10 GPa. Physics and Chemistry of Minerals, 33, 417–425.

Ohashi, Y. (1982) A program to calculate the strain tensor from two sets of unit-cell parameters. In R.M. Hazen and L.W. Finger, Eds., Comparative crystal chemistry, p. 92–102. Wiley, Chichester, U.K.

Ohashi, H., Fujita, T., and Osawa, T. (1982) The crystal structure of the $NaTiSi_2O_6$. Journal of Japanese Association of Mineralogists, Petrologists and Economic Geologists, 77, 305–309.

Ohashi, H., Fujita, T., and Osawa, T. (1983) The crystal structure of $NaGaSi_2O_6$ pyroxene. Journal of Japanese Association of Mineralogists, Petrologists and Economic Geologists, 78, 159–163.

Ohashi, H., Osawa, T., and Tsukimura, K. (1987) Refinement of the structure of manganese sodium dimetasilicate. Acta Crystallographica C, 43, 605–607.

Ohashi, H., Osawa, T., and Sato, A. (1990) Structure of $Na(In,Sc)Si_2O_6$ clinopyroxenes formed at 6-GPa pressure. Acta Crystallographica B, 46, 742–747.

Ohashi, H., Osawa, T., and Sato, A. (1994a) $NaVSi_2O_6$. Acta Crystallographica C, 50, 1652–1655.

——— (1994b) $NaScSi_2O_6$. Acta Crystallographica C, 50, 838–840.

——— (1995) Low-density form of $NaGaSi_2O_6$. Acta Crystallographica C, 51, 2476–2477.

Origlieri, M.J., Downs, R.T., Thompson, R.M., Pommier, C.J.S., Denton, M.B., and Harlow, G.E. (2003) High-pressure crystal structure of kosmochlor, NaCrSi2O6, and systematics of anisotropic compression in pyroxenes. American Mineralogist, 88, 1025–1032.

Prewitt, C.T. and Burnham, C.W. (1966) The crystal structure of jadeite, $NaAlSi_2O_6$. American Mineralogist, 51, 956–975.

Ralph, R.L. and Finger, L.W. (1982) A computer program for refinement of crystal orientation matrix and lattice constraints from diffractometer data with lattice symmetry constraints. Journal of Applied Crystallography, 15, 537–539.

Redhammer, G.J. and Roth, G. (2002) Structural variations in the aegirine solid-solution series $(Na,Li)FeSi_2O_6$ at 298 K and 80 K. Zeitschrift für Kristallographie, 217, 63–72.

——— (2004) Structural variation and crystal chemistry of $LiMe^{3+}Si_2O_6$ Me^{3+} = Al, Ga, Cr, V, Fe, Sc and In. Zeitschrift für Kristallographie, 219, 278–294.

Redhammer, G.J., Ohashi, H., and Roth, G. (2003) Single-crystal refinement of $NaTiSi_2O_6$ clinopyroxene at low temperatures ($298 < T < 100$ K). Acta Crystallographica B, 59, 730–746.

Redhammer, G.J., Amthauer, G., Roth, G., Tippelt, G., and Lottermoser, W. (2006) Single-crystal X-ray diffraction and temperature dependent ^{57}Fe Mössbauer spectroscopy on the hedenbergite-aegirine $(Ca,Na)(Fe^{2+},Fe^{3+})Si_2O_6$ solid solution. American Mineralogist, 91, 1271–1292.

Robinson, K., Gibbs, G.V., and Ribbe, P.H. (1971) Quadratic elongation; a quantitative measure of distortion in coordination polyhedra. Science, 172, 567–570.

Shannon, R.D. (1976) Revised effective ionic radii and systematic studies of interatomic distances in halides and chalcogenides. Acta Crystallographica A, 32, 751–767.

Sheldrick, G.M. (1997) SHELX, programs for Crystal Structure Analysis (Release 97-2). Institüt für Anorganische Chemie der Universität, Tammanstrasse 4, D-3400 Göttingen, Germany, 1998.

Sowa, H. (1994) The crystal structure of $GaPO_4$ at high-pressure. Zeitschrift für Kristallographie, 209, 954–960.

Spek, A.L. (1997) HELENA. Universty of Utrecht, The Netherlands.

Stixrude, L. and Lithgow-Bertelloni, C. (2005) Thermodynamics of mantle minerals—I. Physical properties. Geophysical Journal International, 162, 610–632.

Suzuki, I., Okajima, S., and Seya, K. (1979) Thermal expansion of single-crystal manganosite. Journal of Physics of the Earth, 27, 63–69.

Tribaudino, M., Nestola, F., and Ohashi, H. (2005) High temperature single crystal investigation in a clinopyroxene of composition $Na_{0.50}Ca_{0.50}Cr_{0.50}Mg_{0.50}Si_2O_6$. European Journal of Mineralogy, 17, 297–304.

Vasylechko, L., Pivak, Y., Senyshyn, A., Savytskii, D., Berkowski, M., Borrmann, H., Knapp, M., and Paulmann, C. (2005) Crystal structure and thermal expansion of $PrGaO_3$ in the temperature range 12–1253 K. Journal of Solid State Chemistry, 178, 270–278.

Werner, S., Maximov, B., Schulz, H., Molchanov, V., Vigdorchik, A., and Pisarevskii, Y. (2002) Lattice parameters of $La_3Ga_5SiO_{14}$ as a function of hydrostatic pressure. Zeitschrift für Kristallografie, 217, 460–463.

Wilson, A.J.C., Ed. (1995) International tables for crystallography, Volume C. Kluwer Academic Publishers, Dordrecht, The Netherlands.

Yang, H., and Prewitt, C.T. (2000) Chain and layer silicates at high-tempeature and pressure. In R.M. Hazen and R.T. Downs, Eds., High-temperature and high-pressure crystal chemistry, 41, p. 211–255. Reviews in Mineralogy and Geochemistry, Mineralogical Society of America, Chantilly, Virginia.

Zhang, L., Ahsbahs, H., Hafner, S.S., and Kutoglu, A. (1997) Single-crystal compression and crystal structure of clinopyroxene up to 10 GPa. American Mineralogist, 82, 245–258.

Zhao, Y., Von Dreele, R.B., Shankland, T.J., Weidner, D.J., Zhang, J.Z., Wang, Y.B., and Gasparik, T. (1997) Thermoelastic equation of state of jadeite $NaAlSi_2O_6$: an energy-dispersive Rietveld refinement study of low symmetry and multiple phase diffraction. Geophysical Research Letters, 24, 5–8.

MANUSCRIPT RECEIVED MAY 9, 2006
MANUSCRIPT ACCEPTED OCTOBER 23, 2006
MANUSCRIPT HANDLED BY G. DIEGO GATTA